MARKER-CELL METHOD IN THE DISPLACEMENT OF A LIQUID FROM A CHANNEL WITH A RECESS

G. I. Burdé and I. B. Simanovskii

UDC 532.526

A two-liquid form of the marker-cell method is used to examine the displacement of a liquid from a channel with a rectangular recess.

The usual finite-difference methods cannot be applied to numerical simulation for processes in which one liquid displaces another. The difficulties occur because the density and viscosity at any point are not known in advance and vary as the flow develops on account of the mutual penetration of the liquids.

These difficulties can be overcome in the two-liquid form of the marker-cell method [1-3], which operates with Lagrangian particles (markers), which move through the cells of a net specified in space. The markers play two roles: they indicate the regions of space occupied by each liquid and they also define the density and viscosity in the cells (from the proportions of markers of different types).

Here the marker-cell method is used to examine the displacement of a liquid from a channel with a rectangular recess. This has many practical applications, such as the weathering of salt or coal mines, cementation in oil and gas wells, etc.

We consider the formulation. We assume that in the initial state a channel with a recess is filled with a steadily moving homogeneous liquid, while another liquid begins to be pumped into the inlet at the initial instant. The two liquids are assumed to be viscous, Newtonian, and incompressible, while the flow is planar.

Figure 1 shows the form of the working region and the coordinate axes. The boundaries AH, BC, CD, DE, EF, and FG are solid. The inlet and outlet sections lie reasonably far from the depression, so the velocity distribution in them can be considered as plane-parallel.

The system of equations defining the flow of a mixture of two viscous incompressible liquids differing in density and viscosity is written by the marker-cell method as equations for a homogeneous medium of variable density and viscosity. The two-component nature of the system is reflected in the way the viscosity and density are calculated from the relative contents of the different types of markers. There is then no need to write the equation for the concentration. The equations have the following form for planar flow:

$$\frac{\partial(\rho u)}{\partial t}+\frac{\partial(\rho u^2)}{\partial x}+\frac{\partial(\rho uv)}{\partial y}=-\frac{\partial p}{\partial x}+\frac{1}{\mathrm{Re}}\left\{2\frac{\partial}{\partial x}\left(\mu\frac{\partial u}{\partial x}\right)+\frac{\partial}{\partial y}\left[\mu\left(\frac{\partial u}{\partial y}+\frac{\partial v}{\partial x}\right)\right]\right\}, \tag{1}$$

$$\frac{\partial(\rho v)}{\partial t}+\frac{\partial(\rho uv)}{\partial x}+\frac{\partial(\rho v^2)}{\partial y}=-\frac{\partial p}{\partial y}+\frac{1}{\mathrm{Re}}\left\{\frac{\partial}{\partial x}\left[\mu\left(\frac{\partial u}{\partial y}+\frac{\partial v}{\partial x}\right)\right]+2\frac{\partial}{\partial y}\left(\mu\frac{\partial v}{\partial y}\right)\right\}, \tag{2}$$

$$\frac{\partial u}{\partial x}+\frac{\partial v}{\partial y}=0, \tag{3}$$

where ρ and μ are the dimensionless density and dynamic viscosity, which are defined as the ratios of the dimensional density and viscosity to ρ_1 and μ_1. Here and subsequently, subscript 1 denotes the characteristics of the displaced liquid, while subscript 2 denotes the displacing one. The units of measurement for length, velocity, time, and pressure are respectively the half-width of the channel h, the mean pumping speed U_0, and the quantities h/U_0 and $\rho_1 U_0^2$. The Reynolds number is defined by the mean pumping speed and the characteristics of the first liquid $\mathrm{Re} = U_0 h\rho_1/\mu_1$.

Perm State Pedagogic Institute. Translated from Inzhenerno-Fizicheskii Zhurnal, Vol. 40, No. 4, pp. 631-636, April, 1981. Original article submitted February 29, 1980.

0022-0841/81/4004-0375$07.50

Along with the incompressibility condition (3), we must have a zero value for the Lagrangian derivative of the density with respect to time $d\rho/dt = 0$ in order to ensure the conservation of mass. This relation does not appear in the system of equations, since obedience to it is provided directly in the computation.

The calculation from (1)-(3) consists of two stages. In the first stage, the difference method gives a solution to the equations corresponding to the steady-state flow of a homogeneous liquid. The boundary conditions are then as follows:

$$u = v = 0 \text{ on } BC,\ CD,\ DE,\ EF,\ FG \ \&\ AH, \tag{4}$$

$$u = \frac{3}{2} y(2-y),\ v = 0 \text{ on } AB \ \&\ GH, \tag{5}$$

$$p = 0 \text{ on } AB, \tag{6}$$

$$\frac{\partial p}{\partial x} = -\frac{3}{\mathrm{Re}} \text{ on } GH. \tag{7}$$

In the second stage one considers the flow of a system of two liquids, which begins after we have obtained a steady-state flow for a homogeneous liquid and involves calculating not only the distributions of u, v, and p but also the density and viscosity at each point, which is performed by means of marker movements. The boundary conditions (4)-(6) are used in the previous form, with the addition of conditions for the density and viscosity:

$$\frac{\partial \rho}{\partial n} = 0 \text{ on } BC,\ CD,\ DE,\ EF,\ FG, \tag{8}$$

where n is the normal to the boundary, and

$$\rho = \frac{\rho_2}{\rho_1},\ \mu = \frac{\mu_2}{\mu_1} \text{ on } AB, \tag{9}$$

where condition (7) ceases to be obeyed when the displacing liquid reaches the output section. The pressure and the values of ρ and μ at the outlet are not specified but are computed in the process. The corresponding formulas and the boundary conditions for the pressure at the solid walls will be considered below in the difference implementation.

A divergent difference scheme was used to solve (1)-(3), in which the conservation laws were obeyed for each cell in the rectangular net. The horizontal and vertical components of the velocity were determined at the middles of the vertical and horizontal sides of the cell respectively, while the scalar quantities were related to the centers of the cells in order to write the divergent difference relations (Fig. 1).

We write the finite-difference analog of (1)-(3), where i and j enumerate the vertical and horizontal coordinate lines passing through the centers of the cells (Fig. 1), while n is the number of the time cycle and Δt is the time step:

$$(\rho u)^{n+1}_{i+1/2,j} = (\rho u)^{n}_{i+1/2,j} + \Delta t \left(Q^n_{i+1/2,j} + \frac{p^n_{i,j} - p^n_{i+1,j}}{\Delta x} \right), \tag{10}$$

$$(\rho v)^{n+1}_{i,j+1/2} = (\rho v)^{n}_{i,j+1/2} + \Delta t \left(S^n_{i,j+1/2} + \frac{p^n_{i,j} - p^n_{i,j+1}}{\Delta y} \right), \tag{11}$$

$$\frac{u^{n+1}_{i+1/2,j} - u^{n+1}_{i-1/2,j}}{\Delta x} + \frac{v^{n+1}_{i,j+1/2} - v^{n+1}_{i,j-1/2}}{\Delta y} = 0. \tag{12}$$

Here $Q^n_{i+1/2,j}$, $S^n_{i,j+1/2}$ are expressed by the values of the variables u, v, ρ, and μ in time layer n, while the full form of the finite-difference formulas can be found in [3].

Substitution of the u^{n+1} and v^{n+1} calculated from (10) and (11) into (12) gives an equation of Poisson type for the pressure, which may be solved by Liebman's iterative method with sequential upper relaxation.

The boundary conditions for the difference equations are formulated by means of an additional (fictitious) series of cells outside the boundaries of the working region. We

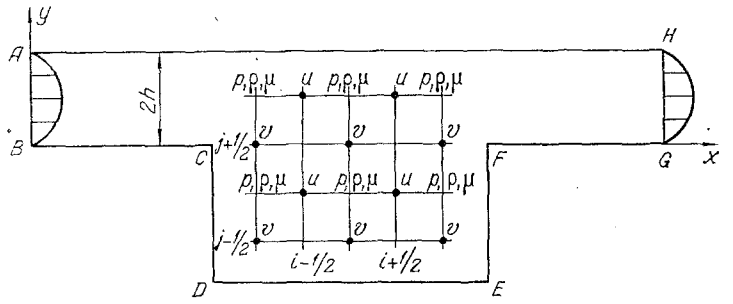

Fig. 1. Working region.

choose the values of ρ, μ, u, v, p in these cells appropriately to meet the boundary conditions and at the same time to provide scope for calculating all the points in the region (including those adjoining the boundary). We consider the corresponding formulas only for cells adjoining the inlet and outlet sections (the formulas for the solid boundaries are discussed in [1-3]).

The equations for the inlet section AB take the form

$$v_{0,j+1/2} = -v_{1,j+1/2}, \tag{13}$$

$$u_{-1/2,j} = u_{3/2,j}, \tag{14}$$

$$\rho_{0,j} = 2\frac{\rho_2}{\rho_1} - \rho_{1,j}, \tag{15}$$

$$\mu_{0,j} = 2\frac{\mu_2}{\mu_1} - \mu_{1,j}, \tag{16}$$

$$p_{0,j} = -p_{1,j}. \tag{17}$$

Equation (13) follows from the second condition in (5), while to obtain (14) we use (5) and the equation of continuity, and (15) and (16) follow from (9), while (17) means that the pressure on the line AB is taken as the origin.

At the fictitious nodes adjoining the outlet section GH, we calculate the values of p, ρ, and μ from the values at some internal nodes via interpolation formulas analogous to those used in [4]. For example, for the density

$$\rho_{k+1,j} = \rho_{k-3,j} - 2\rho_{k-2,j} + 2\rho_{k-1,j}. \tag{18}$$

Here k is the number of the internal vertical row of cells adjoining GH.

Calculations on the flow of a homogeneous liquid involve calculating the fields of u and v from (10)-(11) and conditions of the type of (13) and (14), together with determination of the pressure field by an iterative method by use of the boundary conditions. The density and viscosity fields appearing in the formulas remain constant: at all points $\rho_{i,j} = \mu_{i,j} = 1$.

In calculating the flow of the two-liquid system, we introduce markers moving against the background of the immobile net and serving to determine the density and viscosity fields.

Each cycle of computation involves passing from time layer n to layer n + 1, and it begins with known values for the density, viscosity, and two velocity components, as well as known values for the marker coordinates.

The computations involve determining the pressure field (iterative solution of Poisson's equation), calculation of the velocity fields from (10) and (11), and determination of the new coordinates of the markers from

$$x = x^n + \Delta t u^{n+1},\ y = y^n + \Delta t v^{n+1}$$

(the speeds of the markers are found by interpolation), and calculation of the density and viscosity in each cell from the formulas

$$\rho = \frac{\rho_1 N_1 + \rho_2 N_2}{N_1 + N_2},\ \mu = \frac{\mu_1 N_1 + \mu_2 N_2}{N_1 + N_2},$$

where N_1 is the number of markers in a cell representing the first liquid and N_2 is the number of markers in a cell representing the second.

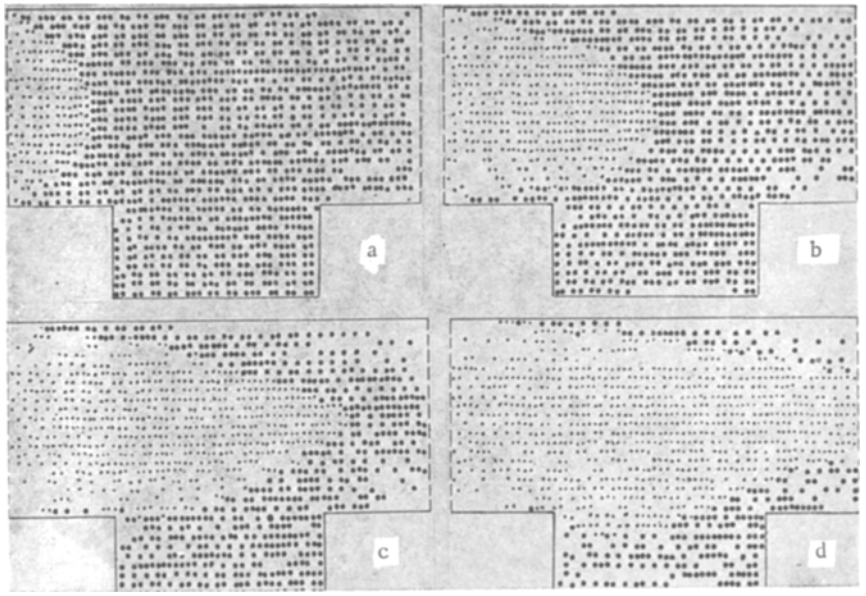

Fig. 2. Stages in the displacement (t_1 = 0.694 (a), t_2 = 2.083 (b), t_3 = 3.473 (c), and t_4 = 6.944 (d)) for Re = 1, $\rho_2/\rho_1 = 1$, $\mu_2/\mu_1 = 2$.

This entire set of calculations is only one step in the iterative process needed to adjust the density and marker-displacement fields (to satisfy the condition $d\rho/dt = 0$) [4].

At each step in this process, the newly determined densities are compared with ρ^n, which are used in calculating the pressures and velocities, and the displacements of the markers are considered untrue if it is found that the newly calculated density distribution does not coincide with the field of ρ^n. Then the markers are returned to the initial positions, but the densities ρ^n and the other characteristics of the liquid are replaced by the newly computed values, and one again calculates the velocities and paths of the markers. This process is continued until the newly calculated density field agrees (within a specified accuracy) with the field of ρ used in calculating the pressures and velocities. Then the new positions for the markers and the fields for all quantities are considered to be true (for time step n + 1), and the cycle is completed.

Stability in the calculation is ensured by choosing the time step as follows:

$$\Delta t = \frac{(\Delta x)^2 (\Delta y)^2}{4\left[(\Delta x)^2 + (\Delta y)^2\right]}.$$

3. The following are some results. It is found that the displacement at low Reynolds numbers is different from that at high ones. At low values of Re, the front of the displacing liquid has a shape such that the displacement occurs primarily at the leading edge of the recess. Figure 2 gives an example of this case, where we show some stages in the displacement for Re = 1, $\rho_2/\rho_1 = 1$, $\mu_2/\mu_1 = 2$. At t = 0, the working region is filled only by markers for the displaced liquid (shown by circles on the figure), while at subsequent instants markers for the displacing liquid (points) begin to appear. The calculations involved more markers than are shown in the figures (we have printed only the coordinates of a quarter of the markers). At high Reynolds numbers, the displacing liquid first fills the central channel, and at this stage the markers for that liquid hardly penetrate into the recess.

Therefore, the displacement is performed more effectively at low Reynolds numbers. This is confirmed by experimental data [5], which show that less time is required to replace the contents of a recess at low Reynolds numbers.

The calculations were performed with various values for the ratios of the densities and viscosities, which showed that the performance in displacement is dependent primarily on the density ratio. If there is a large difference in the densities, the markers for the displacing liquid enter the recess even at fairly high Reynolds numbers. A similar effect has been observed in experiments [5].

Calculations were also performed for liquids of identical density ($\rho_2/\rho_1 = 1$) with various relations between the viscosities ($\mu_2/\mu_1 = 1$, $\mu_2/\mu_1 = 2$, $\mu_2/\mu_1 = 4$), which showed that the degree of displacement even for Re = 1 is almost independent of the viscosity ratio.

NOTATION

x,y, Cartesian coordinates; t, time; u,v, velocity components; p, pressure; h, channel half-width; V_0, mean pumping rate; Re, Reynolds number; $\Delta x, \Delta y$, net steps; N_i, number of markers in a cell.

LITERATURE CITED

1. B. J. Daly, "Numerical study of two-fluid Rayleigh–Taylor instability," Phys. Fluids, 10, No. 2, 297-307 (1967).
2. B. J. Daly and W. E. Pracht, "Numerical study of density-current surges," Phys. Fluids, 11, No. 1, 15-30 (1968).
3. B. J. Daly, "Numerical study of the effect of surface tension on interface instability," Phys. Fluids, 12, No. 7, 1340-1354 (1969).
4. S. Uchida and M. Endo, "On some numerical solutions of the flow through a back-step channel," Mem. Fac. Eng., Nagoya Univ., 27, No. 1, 152-161 (1975).
5. S. I. Bakhtiyarov, "An experimental study of the dynamics of displacement of a liquid from a recess," in: Thermophysics and Physical Hydrodynamics [in Russian], Novosibirsk (1978), pp. 62-67.

STRUCTURE OF A TWO-PHASE EDGE WAKE

P. V. Khrabrov, V. A. Khaimov, and G. S. Shvartsman

UDC 532.62

Experimental results are presented on the structural and kinematic characteristics of the motion of a liquid in an edge wake.

The resistance law for a truncated sphere is used in calculating a two-phase edge wake, e.g., as in wet-steam turbine stages. Extensive evidence has been accumulated on the motion of individual droplets, and this allows one to incorporate the effects of various factors on the resistance coefficients, such as the nonstationary and turbulent nature of the carrying flow, the internal circulation of the droplets, the deformation, etc. At the same time, it remains unclear how far these results are applicable to the motion of droplets in an edge wake with high concentration and velocity gradients. As a consequence, it appears preferable to use the critical Weber numbers, which characterize the stability of droplets of maximum size, and the effects from droplet interaction on the structure of the edge wake.

There are serious difficulties in measuring the local structural and kinematic parameters of a high-speed droplet flow and determining whether one is justified in transferring the laws of motion of single drops to the conditions of an edge wake.

Here we examine some aspects of this problem. We have developed a statistical method of high-speed photography. The essence is a follows. We represent a droplet of diameter d moving with velocity c^{τ} in the median plane of the focal range of a camera (Fig. 1). The camera is fitted with a scan system, and the axis of rotation of the mirror is parallel to the direction of droplet motion. The image of the droplet in the appropriate scale is constructed by the input optical system 1 in the plane of the slot 2, which is conjugate to the axis of rotation of the mirror. Then part of the droplet image cut off by slot 2 is transferred by the lens 3 and the rotating mirror 4 to the film 5. During the exposure, the image of the drop at the film moves along the line AB, whose width along the slot is determined by the size of the droplet, while the angle α is determined by the ratio of the scan speed (line AC) and the speed of the droplet on the appropriate scale (line CB). If the slot width is sufficiently small and a collimated beam is employed, which lies at the optical axis of the camera, the error in imaging the droplet as a sphere is small and may be neglected. The optimum mutual disposition of the slot and the droplet image occurs when

Translated from Inzhenerno-Fizicheskii Zhurnal, Vol. 40, No. 4, pp. 637-644, April, 1981. Original article submitted March 7, 1980.

0022-0841/81/4004-0379$07.50